

# Performance of an InGaN/GaN/AlGaN MSM photodetector

A. HAMDOUNE\*, Z. ALLAM, C. BOUDAUD

Unity of Research "Materials and Renewable Energies", Faculty of Science, University of Abou-bekr Belkaid, P.O. Box 230, 13000, Tlemcen, Algeria

In this paper, an InGaN/GaN/AlGaN visible and ultraviolet (UV) photodetector was studied. Modeling and characteristics were performed using the semiconductor device simulation software SILVACO-TCAD. Energy diagram, internal potential, electric field, and conduction current density were first performed, and then external characteristics simulated. The device exhibited a current of about 1.5 mA for -10 V applied bias; this is in good agreement with the experimental value of current. Under -0.2 V bias; the photocurrent had a value of 22.5  $\mu$ A for a wavelength ranging from 100 nm to 650 nm.

(Received April 25, 2013; accepted January 22, 2014)

**Keywords:** Gallium nitride (GaN), Aluminum gallium nitride AlGaN, Indium gallium nitride InGaN, Visible spectrum, Ultraviolet spectrum, Photodetector

## 1. Introduction

N-nitride semiconductor materials have recently attracted much interest in applications to optical and electronic devices [1]. Wide band gap materials, especially III-V nitride materials, have attracted extensive interest more and more for their applications in making light emitting devices, high-power and high-temperature electronic devices, and ultraviolet detectors. The use of III-V nitrides for photoelectric detector applications is expected to yield high responsivity with low dark currents over a wide range of temperatures. InN, GaN and AlN have direct band gaps of 0.7, 3.4 and 6.2 eV, respectively. Since they are miscible with each other, they form InGaN, AlGaN and InAlN ternaries with respectively 0.7 to 3.4 eV, 3.4 to 6.2 eV and 0.7 to 6.2 eV band gaps range. With AlGaN, we have cutoff wavelengths from 365 to 200 nm; and with InGaN we have wavelengths from 1770 to 365 nm [2].

MSM photodiodes are comprised of two back-to-back Schottky diodes by using an interdigitated electrode configuration on top of the active light collection region.

These photodetectors cannot operate at a zero bias. Their main interest is the high gain. Due to their low capacitance per unit area, the response for the same material is greater by several orders of magnitude than that of other photodetectors. On the other hand, their performances (band-width, rate of UV/Visible rejection, detectivity, and noise) are often degraded.

With the electron beam lithography, the width and spacing of the electrodes can be made with submicron dimensions, which considerably improve the response time of the device. The biggest drawback of MSM photodetectors is their intrinsic low responsivity. MSM detectors exhibit low photoresponsivity mainly because the metallization for the electrodes shadows the active light collecting region.

In new technologies, the need for high quality materials AlN, GaN, InN, and their alloys AlGaN, and InGaN, is an essential condition. The basic research is very important to understand the mechanisms of growth and thus improve the quality of materials controlling the growth conditions and also exploring new ways to implement the ability of modern growth [3].

## 2. Experimental procedure and structure design

"Atlas" is a simulator 3D and 2D device based on semiconductor physics. It predicts the electrical behavior of semiconductor structures specified and provides insights into the physical mechanisms associated with the internal operation of the devices. Atlas can be used independently or as a tool in the kernel environment simulation called VWF (Virtual Wafer Fab.) of SILVACO, as shown in Fig. 1. In order to envisage the impact of the variables of process on the behavior of the device, simulation was attached to the simulation of the process model and the extraction by SPICE (Simulation Program with Integrated Circuit Emphasis) [4].

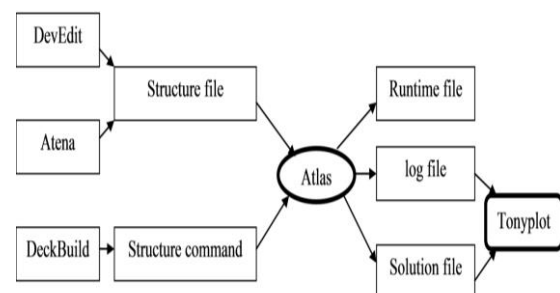


Fig. 1. Inputs and outputs of Atlas.

The schematic structure of InGaN/GaN/AlGaN visible and UV photodetector is shown in Fig. 2; it was simulated using ATHENA and ATLAS in SILVACO TCAD device simulator. However, thin GaN window layer, is typically strained due to lattice mismatch with InGaN and AlGaN layers and hence, generate substantial piezoelectric polarization.

Device model is established based on the nature of GaN, AlGaN and InGaN, and all of the simulated results are on the basis of the drift-diffusion equations.

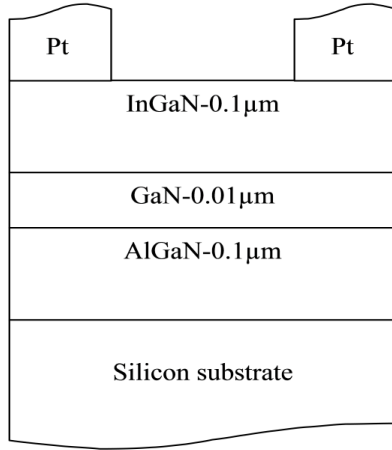


Fig. 2. Schematic structure of studied photodetector with Pt electrodes.

Respectively for  $\text{Al}_x\text{Ga}_{1-x}\text{N}$  and  $\text{In}_x\text{Ga}_{1-x}\text{N}$  compounds, bandgaps are given by equations (1) and (2), using Vegard's.

$$E_g(x) = x \times E_g(\text{AlN}) + (1-x) \times E_g(\text{GaN}) - b \times (1-x) \times x \quad (1)$$

$$E_g(x) = x \times E_g(\text{InN}) + (1-x) \times E_g(\text{GaN}) - b \times (1-x) \times x \quad (2)$$

Here:  $E_g(\text{AlN}) = 6.2$  eV,  $E_g(\text{GaN}) = 3.42$  eV, and  $b = 1$  [5] for  $\text{Al}_x\text{Ga}_{1-x}\text{N}$  alloy;  $E_g(\text{InN}) = 0.7$  eV and  $b = 1.43$  eV for  $\text{In}_x\text{Ga}_{1-x}\text{N}$  alloy [6].

The device structure consisted of 0.3 μm thick silicon substrate, 0.1 μm thick undoped AlGaN epitaxial layers grown on silicon substrate by metal organic chemical vapor deposition (MOCVD) at 1100°C [7], 0.01 μm thick GaN layer grown at low temperature (550°C), and 0.1 μm of n-doped thick InGaN with a concentration of  $1 \times 10^{19} \text{ cm}^{-3}$ , grown at high temperature (1050°C). Platinum (Pt) electrodes of 250 nm thicknesses were then deposited on InGaN layer by RF magnetron sputtering.

The ion implantation method has been used because it enables precise control of doping profile, followed by annealing required to activate the dopants and reduce implant-induced disorders [8].

The energy band diagram, as shown in Figure 3, has been simulated using BLAZE tool, which is interfaced with ATLAS. This is a general purpose 2-D devices

simulator for III-V, II-VI materials, and devices with the position dependent band structure (i.e., heterojunctions) [3]. Energy band diagram and net doping of MSM UV photodetector are respectively illustrated by Figs 3 and 4.

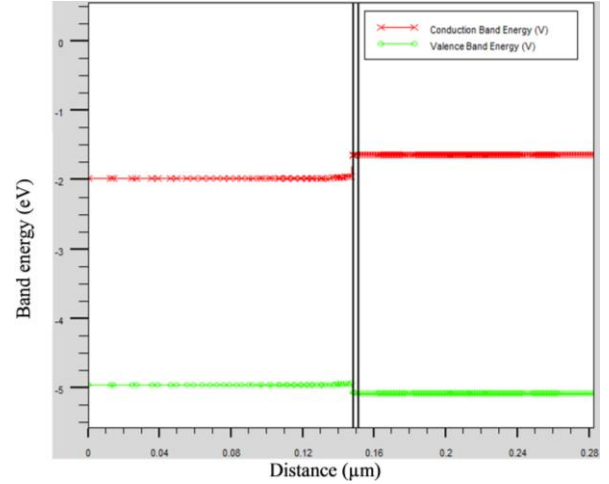


Fig. 3. Energy band diagram.

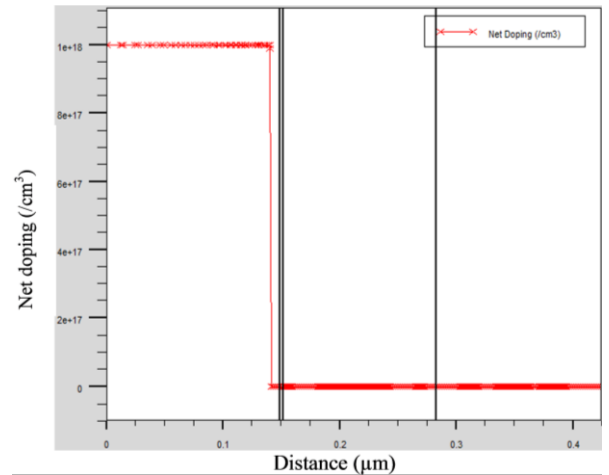


Fig. 4. Net doping within the structure.

### 3. Results and discussion

Two-dimensional numerical simulation of the InGaN/GaN/AlGaN detector was carried out using ATLAS software. A program was developed separately in DECKBUILD window interfaced with ATLAS for calculating different characteristics of the photodetector. The simulation included the solution of five decoupled equations using Newton iteration method. Carrier and doping densities were calculated using Fermi-Dirac statistics. For extracting the electrical characteristics; the optical, SRH and Auger recombination processes were taken into account. The different recombination rates are given as follows:

$$R_c^{opt} = C_c^{opt} (pn - n_i^2) \quad (3)$$

$$R_{SRH} = \frac{pn - n_i^2}{\tau_{p0} \left[ n + n_i \times \exp\left(\frac{E_t}{kT}\right) \right] + \tau_{n0} \left[ p + n_i \times \exp\left(-\frac{E_t}{kT}\right) \right]} \quad (4)$$

$$R_{Auger} = C_n (pn^2 - nn_i^2) + C_p (p^2n - pn_i^2) \quad (5)$$

$$R_{surf} = \frac{pn - n_i^2}{\tau_p^{eff} \left[ n + n_i \times \exp\left(\frac{E_t}{kT}\right) \right] + \tau_n^{eff} \left[ p + n_i \times \exp\left(-\frac{E_t}{kT}\right) \right]} \quad (6)$$

Here  $C_c^{opt}$  is the capture rate of carriers;  $C_n$  and  $C_p$  are Auger coefficients for electrons and holes respectively;  $n$  and  $p$  are electron and hole equilibrium concentrations;  $E_t$  is the energy level of traps;  $n_i$  is intrinsic concentration of carriers;  $\tau_{n0}$  and  $\tau_{p0}$  are SRH lifetime of electrons and holes respectively;  $\tau_n^{eff}$  and  $\tau_p^{eff}$  are effective life times of electrons and holes, respectively [9].

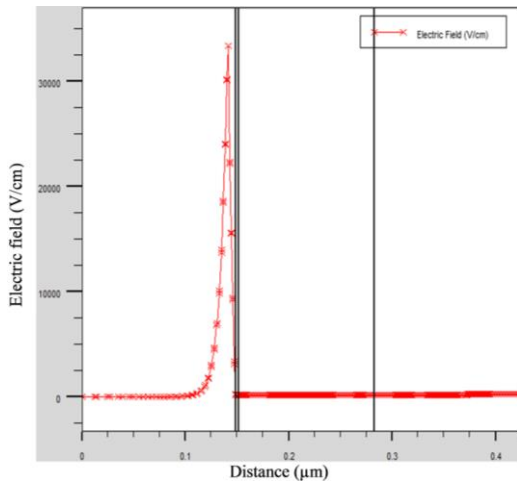


Fig. 5. Electric field profile without external biasing.

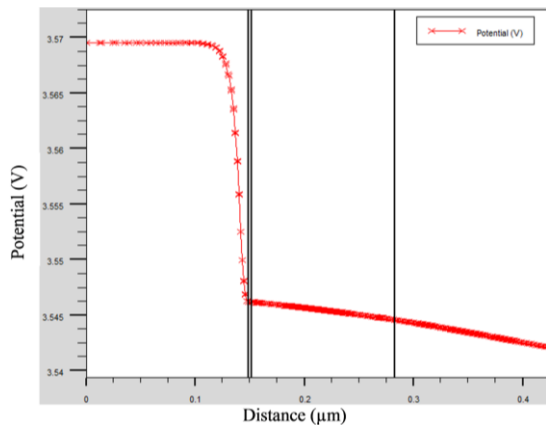


Fig. 6. Internal potential.

The III-nitrides internal polarization has a piezoelectric character. This effect is defined as the creation of an electric field due to a mechanical deformation. It is due to a lack of symmetry in the crystal structure, to the nature of the chemical bonds highly ionic, and to the distortion in the crystal (due to lattice mismatch between the material and the substrate, for example). The piezoelectric polarization is not necessarily oriented in the same direction as the internal polarization; it depends on the material properties [10].

The electric field and the potential across the structure, as shown respectively in Figs. 5 and 6, confirm the presence of barriers at the interfaces despite the largest electric field in n-type InGaN, which promotes separation of photo-generated carriers. Finally, the carrier concentration in the layer results in a phenomenon of accumulation of electrons at the interface.

In the interface metal/semiconductor, there is a potential barrier for electrons due to the difference in work functions between the metal and the semiconductor. This causes the formation of a potential well in the smaller-gap material; in this well, electrons are transferred from the donor layer. The heterojunction is characterized by the energy-discontinuity between the conduction bands of the two materials; the electron transfer to the quantum wells is even better than the discontinuity of the conduction bands is large. In addition, the electrical transport properties are better for a smaller gap of the channel. The simulated current density is shown in Fig. 7.

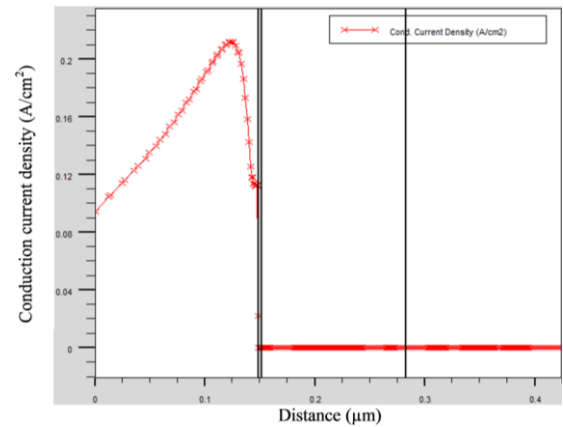


Fig. 7. Conduction current density.

We observe a high value of current density in InGaN layer: 0.215 A/cm<sup>2</sup> for reverse bias up to 0.5 V.

The detection layer has the smallest gap, and therefore the current density is greater. Because of its small gap, most photons arriving on InGaN have energy greater than or equal to the gap producing a high current density. When the gap increases, the voltage increases but also fewer photons have sufficient energy to be absorbed, reducing the current density of photodetector.

The mechanism of optical gain in InGaN quantum well of UV photodetector is not yet fully understood because the InGaN alloy admits a wavelength of about 726

nm for a molar fraction of indium of 0.5, which corresponds to the red color.

It can be strongly affected by non-uniform distribution. Internal bias fields tend to separate quantum confined electrons and holes, which reduces the optical gain and spontaneous emission. However, the screening of the electrons and holes is provided to remove bias fields at high current operation [11].

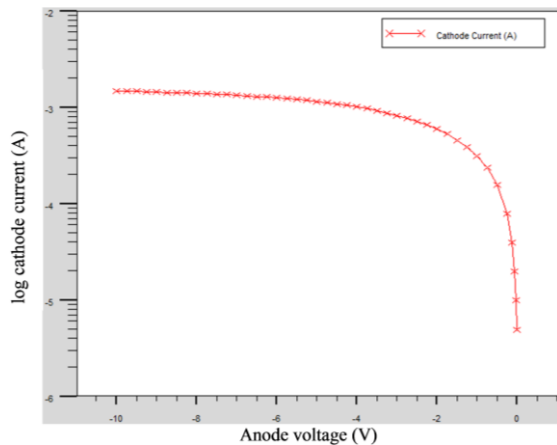


Fig. 8. Reverse bias I-V characteristic.

We find a current of about 1.5 mA for -10 V applied bias; this is in good agreement with the experimental value of current.

A Schottky contact is formed between InGaN and Pt. It is confirmed by current-voltage (I-V) and capacitance-voltage (C-V) methods of measurements [12]. The diode has an apparently rectifying current characteristic.

The variation of photocurrent as a function of wavelength at a bias voltage of -0.2 V is shown in Fig. 9.

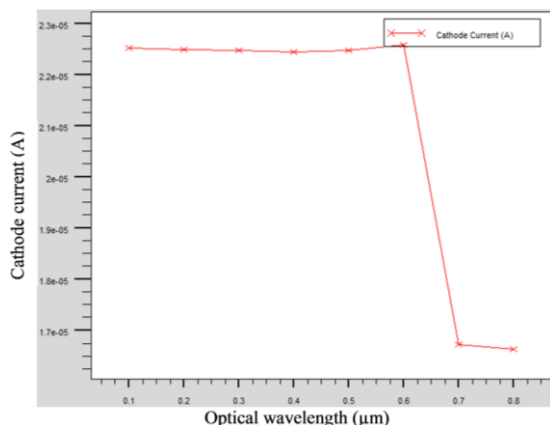


Fig. 9. Photocurrent as a function of optical wavelength, for -0.2 V bias.

We can optimize the performance of the device by changing doping concentration and dimensions of the device for high bandwidth performance.

This structure offers a wide spectrum of response from the visible to the UV, and it blind at wavelengths above 650 nm. It is particularly suitable for applications in the ultraviolet and visible from 100 nm to 650 nm with a current of  $2.25 \times 10^{-5}$  A; this is a good result, probably due to the use of InGaN and to the silicon substrate in the structure of photodetector.

#### 4. Conclusion

In this paper, we studied an InGaN/GaN/AlGaN photodetector device. Modeling and simulation were performed by using ATLAS-TCAD simulator. Energy diagram, internal potential, electric field, and conduction current density were performed.

The device exhibited a very good current of about 1.5 mA. Under -0.2 V bias; the photocurrent demonstrated a value of 22.5  $\mu$ A for a wavelength ranging from 100 nm matching the far ultraviolet to 650 nm (corresponding to red color).

With their gaps, GaN and AlGaN only detect wavelengths located in the ultra-violet; but with a layer of InGaN, the device can detect wavelengths much higher. With the adequate molar fraction of indium in the InGaN alloy, one can limit detection to the desired wavelength.

The simulation and modeling described in this work can be used for optimizing the existing photodetectors and developing new structures.

#### References

- [1] Ping-Chuan Chang, Chin-Hsiang Chen, Shoou-Jinn Chang, Yan-Kuin Su, Chia-Lin Yu, Bohr-Ran Huang and Po-Chang Chen, Thin Solid Films. **498**, 133 (2006).
- [2] M. B. Reine, A. Hairston, P. Lamarre, et al, Proc. SPIE, 6119, 2006, p. 1 – 15.
- [3] Pierre Masri, Surface Science Reports. **48**, 1 (2002).
- [4] ATLAS User's Manual Version 5.10.0.R, SILVACO International, Santa Clara, CA 95054 (2005).
- [5] D. L. Pulfrey, B. D. Nener, Solid-State Electronics. **42**, 1731 (1998).
- [6] J. Wu, W. Walukiewicz, K. M. Yu, J. W. Ager III, E.E. Haller, H. Lunad W. J. Schaff, Appl. Phys. Lett. 4741 – 4743 (2002).
- [7] Guozhen SHEN, Di CHEN, Front. Optoelectron. China. **3**, 125 (2010).
- [8] M. Katsikini, et al. Journal of Applied Physics. **94**, 4389 (2003).
- [9] A. D. D. Dwivedi, A. Mittal, A. Agrawal, P. Chakrabarti, Infrared Physics & Technology. **53**, 236 (2010).
- [10] L. Liu, J. H. Edgar Materials Science and Engineering R. **37**, 61 (2002).
- [11] A. V. Dmitriev, A. L. Oruzhenikov. MRS Internet J. Nitride Semicond. Res. **1**, 46 (1996).
- [12] Ja-Soon Jang, Donghwan Kim, Tae-Yeon Seong. J. Appl. Phys. **99**, 073704 (2006).

\*Corresponding author: ahamdoune@gmail.com